

INSTITUTE OF PLASMA PHYSICS

NAGOYA UNIVERSITY

Observation of Drift Motion of
a Collisional Plasma in Cross Fields

Altaf Hussain

IPPJ-221

April 1975

RESEARCH REPORT

NAGOYA, JAPAN

Observation of Drift Motion of
a Collisional Plasma in Cross Fields

Altaf Hussain

IPPJ-221

April 1975

Further communication about this report is to be sent to the Research Information Center, Institute of Plasma Physics, Nagoya University, Nagoya, Japan.

Abstract

The drift velocity of particles undergoing $\vec{E} \times \vec{B}$ rotation in a collisional plasma is investigated by test wave technique and Langmuir probe. The velocity determined by probe is corrected by including effect of cylindrical geometry and finite Larmor radius effect. From the B dependence of the corrected velocity and the drift velocity determined by test wave, the ion-neutral collision cross section is determined which is found to be in disagreement with the value given by the current data. This disagreement is attributed to an inappropriate collision cross section at low energy at which small angle scattering events are frequent. It is proposed that in events in which there is a loss of particle drift velocity, we should use the so-called "slowing down cross section" σ_s , rather than the total cross section.

1. Introduction

A weakly ionized plasma column which has a radial electric field E_r and is immersed in an axial, uniform magnetic field is subject to large number of instabilities. Due to the presence of E_r , the particles drift azimuthally. The ions, being heavier and experiencing greater frictional force with the neutrals, lag behind the electrons, resulting in charge separation in such a fashion as to cause instability. As the ion motion plays an important role in causing an instability, information regarding the ion motion must be very accurately known. For this purpose the most common method adapted is that of the measurement of electric field and other plasma parameters by Langmuir probe. But the information collected by this method are not reliable. Particularly in an unstable plasma, the E_r measurement by Langmuir probe is vulnerable to many errors. A collisional plasma makes the whole affair more complex. At low energy, in most cases, the ion-neutral collision cross section is not available in literature and the usual extrapolation method (from the current available data)¹⁾ does not give the appropriate cross section for the purpose and, therefore, is not trustworthy. Further complexity of the problem stems from the fact that the cylindrical geometry and, in a low magnetic field case, the ion Larmor radius must be taken into account. The usual theoretical models neglect the finite Larmor radius effects which may contribute significantly to the phenomena occurring in plasma. Very recently Horikoshi et al.²⁾ have shown the contribution of finite Larmor radius

and cylindrical effects in a collisional plasma.

In this paper the results of the experiment conducted in a partially ionized, low temperature plasma are presented. Cylindrical effects and finite Larmor radius correction are duly taken into account. The azimuthal velocity of the particles is determined by Langmuir probe and by test wave technique. The effects of collisions are studied and a more appropriate collision cross section at low energy is suggested. Sec.2 is devoted to theory of the method used as a test wave technique tool for the measurement of the drift velocity. Sec.3 deals with the plasma device and the experimental techniques employed and the results are given in Sec.4. Sec.5 contains discussion and the concluding remarks are presented in Sec.6.

2. Theory of Method

The electrostatic ion waves propagating across the magnetic field has been experimentally investigated by Hirose et al.,³⁾ Ault et al.⁴⁾ and Ohnuma et al.⁵⁾ in the frequency range $\omega \gtrsim \Omega_{ci}$. Low frequency ion waves in an inhomogeneous plasma are theoretically investigated by D'angelo⁶⁾ and Chen⁷⁾ for $\omega \ll \Omega_{ci}$. Very recently Wong and Jassby⁸⁾ have investigated the interaction between particles under going $\vec{E} \times \vec{B}$ rotation and Kelvin-Helmholtz instability across a magnetic field in a collisionless plasma using a test wave technique, but so far, to the author's knowledge, this problem has not been treated in a collisional plasma.

In our experiment ion acoustic wave was used as a test

wave tool in a collisional plasma. The wave was excited parallel and antiparallel to the direction of $\vec{E} \times \vec{B}$ rotation of the plasma and from the difference in the propagation velocity in the two directions plasma drift velocity was calculated. In a quasineutral, low density, partially ionized plasma which is immersed in a uniform magnetic field, the dispersion relation of the test wave is given by

$$\omega^2 - (2k_y V_{0yi})\omega + k_y^2 (V_{0yi}^2 - V_{si}^2 + C_s^2) + \Omega_{ci} k_y (V_{oye} - V_{cyi}) = 0 \quad (1)$$

$$\text{where } V_{0yi} = \frac{(\Omega_{ci} \tau_i)^2}{1 + (\Omega_{ci} \tau_i)^2} \left\{ -\frac{E_x}{B} + \frac{KT}{B} \frac{V_n}{n} \right\}; \quad V_{si} = \left(\frac{KT_i}{m_i} \right)^{1/2};$$

$$C_s = \left(\frac{KT_e}{m_i} \right)^{1/2}$$

Keeping in view our experimental conditions, the collisions between charged particles have been neglected while ion-neutral collisions have been taken into account. Applying the assumptions $\Omega_{ce} \gg \omega \gg \Omega_{ci}$ and after some algebraic simplifications, the two roots of Eq.1 are given by

$$\omega = k_y V_{oyi} \pm k_y C_s \quad (2)$$

which is an ion acoustic wave modified by the plasma rotation. $k_y V_{oyi}$ is the rotational angular frequency of the plasma at radius r_0 which introduces Doppler shift in the

propagation frequency. Therefore, when the wave is travelling in the direction of plasma rotation, its phase velocity is given by $(C_s - V_{0yi})$ while in the opposite direction by $(C_s + V_{0yi})$ as shown by Eq.2. As explained in the next section, the wave was excited by a tungsten wire and received by a receiver — a tungsten wire with the dimensions of the exciter. The signals from the exciter and receiver were fed to an interferometer whose output was displayed on CRO. If the signals of exciter and receiver can be represented by

$$f(t) = Ae^{i\omega t}$$

and $g(t) = Be^{i(\omega t - kx)}$

the output of interferometer is given by

$$\begin{aligned} I &= \frac{1}{T} \int_0^T AB e^{i\omega t} e^{-i(\omega t - kx)} dt \\ &= AB e^{ikx} \end{aligned}$$

$$\text{Re } I = AB \cos kx$$

and $kx = \frac{\omega x}{V_{0yi} \pm C_s}$

where x is the separation between exciter and receiver and is accurately known. Keeping x constant, the wave is excited, sweeping the frequency from 100 kHz to 5 MHz, and two wave patterns, parallel and antiparallel to the direction of $\vec{E} \times \vec{B}$ rotation of plasma, are obtained (Fig.3). From these wave

patterns, dispersion curve, as shown in Fig.4, is obtained. It is seen that the phase velocity in the direction of $\vec{E} \times \vec{B}$ rotation of plasma is larger than in the opposite direction — a result confirming the above considerations. To further certify that, for $\omega \gg \Omega_{ci}$, the wave propagation velocity equals the ion acoustic velocity, the wave velocity was investigated in He and Ar. The velocity in He was found to be nearly three times velocity in Ar showing the mass dependence in agreement with the ion acoustic wave. During the course of the experiment the ion cyclotron frequency for Ar was kept less than 25 KHz.

3. Experimental Set-up

3.1. The experiments are conducted in a Penning discharge. The stainless steel discharge tube is about 160 cm long and 12.5 cm in radius with an annular ring anode at the center as shown in Fig.1. The plasma is produced in argon by an indirectly heated oxide coated cathode 6 cm in diameter. Measuring ports were located nearly at the center of the discharge tube, separated azimuthally through 90° intervals through which probes and exciter and receiver were introduced to the plasma. Mainly the experiments were conducted in argon but to elucidate ion mass effect, hydrogen and helium gases were also used.

All the measurements were made in high pressure $1.0 \sim 6.0 \times 10^{-3}$ Torr and low magnetic field regime. Mirror field geometry (mirror ratio 2:1) is used with a field strength ranging from 30 G to 300 G at the point where all measurements

were made. The plasma density is on the order of 10^{10} cm^{-3} , T_e is 1 ~ 3 eV, T_i is very low, nearly an order less than T_e and the ion plasma frequency is 3.3 MHz. The discharge voltage V_d is 40 ~ 70 V and discharge current is varied from 100 to 700 mA.

3.2. Wave Excitation

The wave is excited by a single tungsten wire 0.5 mm in diameter and 3 cm in length and is received by a wire of the same dimensions biased negatively with respect to plasma. Both the exciter and receiver, which are aligned parallel to the magnetic field (Fig.2), are movable radially and one of them is also movable azimuthally so that the wave can be excited at any desired position or in any direction, clockwise or anticlockwise. To study the wave propagating azimuthally, the azimuthal spacing between exciter and receiver is kept sufficiently small as compared with their radial distance from the plasma axis. For one set of measurement, this separation is kept constant and frequency is swepted from 100 kHz to 5 MHz. The transmitted and received signals are fed to an interferometer whose output, as a function of frequency is displayed on CRO. From the two consecutive peaks of output patterns, as shown in Fig.3, the frequency difference and consequently wave velocity is calculated by the relation

$$\frac{\Delta\omega_1 - \Delta\omega_2}{2\pi} \times x = 2 V_d$$

where $\Delta\omega_1$ and $\Delta\omega_2$ are the frequency differences calculated from the wave patterns obtained. By launching waves parallel and antiparallel to the direction of $\vec{E} \times \vec{B}$ rotation of plasma, we get the azimuthal drift velocity, V_{oyi} , of ions.

4. Results

The azimuthal phase velocity is determined by the deformation of the initially launched sine waves. Typical examples of the output of interferometer are shown in Fig.3(a) for several exciter-receiver spacings with magnetic field being constant while trace (b) depicts the change in the output of the interferometer when the positions of exciter and receiver are interchanged. It can be seen that the periodicity of the signals, as a function of " ω ", is different in the two cases due to azimuthal motion of ions. From this difference in periodicity, the azimuthal drift velocity of ions can easily be calculated. Fig.5 summarizes the azimuthal velocity measurements as a function of radius. It is seen that the azimuthal velocity increases with radius depicting a constant frequency of rotation of the plasma column as a solid body. The direction of ion motion is along $\vec{E} \times \vec{B}$ drift which is opposite to the direction of ion motion due to pressure gradient. Fig.6 shows the radial electric field determined by the space potential which in turn is calculated from the current-voltage probe characteristics. From the semi log plot of the probe characteristics, we can determine the space potential as well as electron temperature.

5. Discussion

The curves in Fig.7 show the azimuthal velocity of plasma. The one determined by the wave technique is shown by the curve "a" while the other, calculated by radial electric field which does not include collision is shown by curve "c". We observe a large discrepancy in the results which is largely due to ion Larmor radius and the collisional effects. It has been shown by Horikoshi et al.²⁾ that the due consideration of finite Larmor radius and cylindrical effects modifies the azimuthal velocity. The new velocity with which the particles are drifting is given by

$$r\omega = \frac{r\Omega_{ci}}{2} \left\{ 1 - \left(1 + \frac{4\omega_{E \times B}}{\Omega_{ci}} \right)^{1/2} \right\}$$

where Ω_{ci} is the ion cyclotron frequency. The curve "b" is the corrected azimuthal velocity without collisions, including the effect of finite Larmor radius. Even taking into account the cylindrical effects we see that the discrepancy is not removed and the two curves do not coincide. Concerning the effect of pressure gradient, we find from Eq.1 that this effect is opposite to that of $\vec{E} \times \vec{B}$ drift. This term, which is usually neglected by many experimentalists, cannot be neglected unless

$$\frac{V_p}{V_{\vec{E} \times \vec{B}}} = \frac{T_i/\lambda}{E_r} \ll 1$$

where V_p is the pressure gradient drift velocity and " λ " is the plasma scale length. Under our experimental conditions, for instance, at $B = 50$ G, $\lambda = 5.8$ cm, $E_r = 0.2$ V/cm and if $T_i \approx 0.1$ eV, $\frac{T_i/\lambda}{E_r} \approx \frac{1}{10}$. Therefore, pressure gradient term can be neglected and the noncoincidence of the two curves is not due to the neglect of the pressure gradient term. Now under the present situation all the discrepancy must be attributed to the collisional effect. In a collisional case, too, the finite Larmor radius and cylindrical effects play important roles and may modify the effect of collisional factor in Eq.1.

Horikoshi et al.⁹⁾ very recently have tackled a similar problem concerning the rotational motion of a cylinder of a collisional plasma starting with the Boltzmann's equation in stationary state

$$m(\vec{\nabla} \cdot \vec{V})\vec{V} = e(\vec{E} + \vec{V} \times \vec{B}) - \nabla(nKT)/n - v m \vec{V}$$

This equation is solved in cylindrical geometry including collisions and, by using computer, curves are plotted between normalized velocities $\frac{V_\theta(v)}{V_\theta(0)}$ and normalized collision frequency $T(= \frac{v}{\Omega_c})$ taking $A(= \frac{\omega_r \vec{E} \times \vec{B}}{\Omega_c})$ as a parameter as shown in Fig.8. The value of A can easily be determined from the experimental data. In Fig.7, curve "b" is the corrected azimuthal velocity (including the ion Larmor radius correction) which does not include collisions and curve "a" is the velocity which includes collisional effects. $\frac{V_\theta(v)}{V_\theta(0)}$ can be determined from these curves at the corresponding magnetic

fields. Knowing $\frac{V_g(\nu)}{V_g(0)}$ and A, T can be determined from the curves in Fig.8, which, knowing magnetic field, gives us the collision frequency ν . A curve was plotted between ν and T. As ν does not depend on B we should expect this curve to be a straight line with zero slope but what we obtained was a straight line with a non-zero slope, indicating a systematic error in the determination of E_x due to unreliable Langmuir probe measurements. Keeping this fact in view E_x was multiplied by a constant K and same procedure, as described above, was followed until a straight line, with zero slope, between ν and T was obtained. This value of K comes about to be 1.7 and the collision frequency calculated in this way is less than the collision frequency determined by the extrapolation method from the current available data.

Now to understand this discrepancy which appears in our results let us consider a collision between two particles in which the energy of the particles does not change and the scattering angle is θ . In this case, the particle velocity in the initial direction is slowed down by $v(1 - \cos\theta)$. If the scattering probability is uniform in all directions, i.e., the differential scattering cross section is independent of θ , the particle is, in average, slowed down by v or, in other words, the particle loses all its velocity component in the initial direction. In general, we can safely employ the equation of motion with a collision term $-\nu\vec{v}$, where ν is the collision frequency directly obtained by the slowing down cross section σ_s , which is given by¹⁰⁾

$$\sigma_s = \int (1 - \cos\theta) \sigma(\theta) d\Omega .$$

Now back to our experiment. To obtain the slowing down cross section we must know the functional form of $\sigma(\theta)$. In the low energy region of $E \lesssim 1$ eV the total cross section consists of two main parts, i.e., elastic cross section and charge transfer cross section. The θ dependence of the former at low energy is not available in the current data. Therefore if we assume that it depends weakly on the scattering angle, then as a result, the slowing down cross section will be nearly equal to the elastic cross section as obtained from the current data. On the other hand, for the charge transfer process, σ_c depends on the relative velocity v_r between a charged and a neutral particle¹¹⁾ as

$$\sigma_c^{1/2} = a - b \ln v_r$$

where a and b are constants. As v_r is expressed in terms of velocities of neutral and charged particles, v_1 and v_2 , and the angle θ between them as

$$v_r^2 = v_1^2 + v_2^2 - 2v_1v_2\cos\theta$$

we can obtain, in principle, σ_c as a function of θ . For simplicity, we assumed $v_1 = v_2$, expressed σ_c as a function of θ , determined the constants a and b and obtained the slowing down cross section from the current data. The

results are summarized in Table 1. From these results, it can be concluded that in the low energy region of $E < 1$ eV where charge transfer cross section is quite large, the experimentally determined total collision cross section is quite close to the calculated slowing down cross section. As mentioned before, it has been assumed that elastic scattering cross section depends weakly on the scattering angle θ . But in case of helium from the current data,^{12,13)} we can get the differential cross section $\sigma(\theta)$ which is quite large at small scattering angle. If at low energy argon also shows the same trend, then the slowing down cross section will be quite smaller than the elastic cross section and the results in Table 1 will show still better agreement. Therefore, at low energy in small angle scattering case in which there is only a small loss of directed particle velocity, we must use the so-called slowing down cross section which is the more appropriate quantity.

In arriving at the results just described, E_r has been multiplied by a comparatively larger factor of $K = 1.7$ which, at the first glance, may not appear to be justified, needs some more considerations.

The determination of E_r by Langmuir probe is subject to large errors and in unstable plasma, particularly, the determination of correct value is quite difficult. In spite of this difficulty the value of $K = 1.7$, which we have used to remove the systematic error in E_r , is quite large. It stems from the fact that to make the problem a bit simpler, we have considered only the ion motion and neglected that of

Table 1

Temperature (eV)	cross section from the current data ($\times 10^{-15} \text{ cm}^2$)			calculated slowing down cross section ($\times 10^{15} \text{ cm}^2$)			experimentally determined total cross section ($\times 10^{-15} \text{ cm}^2$)
	elastic	charge transfer	total	elastic	charge transfer	total	
1	4.8	4.7	9.5	4.8	1.19	6.99	1.77
0.3	5.3	4.95	10.25	5.3	1.31	6.61	3.04
0.1	6.0	5.27	11.27	6.0	1.36	7.36	5.3

electrons. In a plasma, due to E_r , the electrons drift quickly while ions, being heavier and suffering large finite Larmor radius effect, lag behind. This produces a charge separation in the azimuthal direction which decelerates the electrons while slightly increases the velocity of ions. Therefore if electron drift is also considered, a small increase in ions velocity will ultimately reduces the value of K.

In Fig.7 "x" is the separation between the exciter and receiver and, to determine the ion azimuthal velocity, was kept 1 cm. Every precaution was taken to measure this separation quite accurately but even a small error in its measurement will cause larger error in the results. For instance an error of 1 mm will effect the result by 10 %. Such considerations will fairly reduce the value of K within the acceptable limits.

Conclusion

Experimental data show that the collision cross section determined experimentally does not agree with the one given in literature. The difference between the two is largely removed when instead of total collision cross section slowing down cross section is used. In fact in collisions in which particles suffer a change in their directed velocity, slowing down cross section is the most appropriate quantity and is fairly less than the total collision cross section. Particularly, in the analysis of low temperature plasma motion, as in the experiments involving $\vec{E} \times \vec{B}$ or pressure gradient

drifts, in which charge transfer cross section cannot be neglected as compared with elastic collision cross section, instead of total collision cross section slowing down cross section should be used.

Moreover, in most experiments, the effects of finite Larmor radius and cylindrical geometry are not negligible and, where necessary, should be taken into account. Particularly, in plasmas immersed in a low magnetic field where $\frac{\omega_{\pm}^2}{E \times B}$ is quite large, these effects are very important and Ω_{ci} should be duly considered. In this paper these effects are taken into account with satisfactory results.

Acknowledgements

It is a pleasure to thank Drs. G. Horikoshi and T. Kuroda for their kind guidance, encouragement and valuable discussions during the course of the experiments and their commenting upon the manuscript. Thanks are also due to Mr. K. Satoh of the National Laboratory for High Energy Physics for some helpful discussions.

References

1. W. H. Crammer, J. Chem. Phys. 26 (1957) 1272
2. G. Horikoshi, A. Hussain and T. Kuroda, IPPJ 210
3. A. Hirose, I. Alexwff and W. D. Jones, Phys. of Fluids 8 (1970) 2039
4. E. Ault and H. Ikezi, Phys. of Fluids 13 (1970) 2879
5. T. Ohnuma, S. Miyake, T. Sato and T. Watari, Phys. Rev. Letters 10 (1970) 541
6. N. D'Angelo, Phys. of Fluids 6 (1964) 592
7. F. F. Chen, Phys. of Fluids 7 (1964) 949
8. A. Y. Wong and D. L. Jassby, Phys. Rev. Letters 29 (1972) 41
9. G. Horikoshi, A. Hussain and T. Kuroda, IPPJ, (in press)
10. B. A. Trubnikov, Reviews of Plasma Physics, Vol.1
11. L. A. Sena, J. Exp. Theor. Phys. 9 (1939) 1320
12. D. C. Lorentz and W. Aberth. Phys. Rev. 139 (1965) 1017;
144 (1966) 109
13. D. C. Lorentz, W. Aberth and V. W. Hesterman, Phys. Rev. 147 (1966) 849

Figure Captions

- Fig. 1 Experimental arrangement.
- Fig. 2 Block diagram of electronic apparatus.
- Fig. 3 Output of interferometer at $B = 47$ G. In trace (a) each track shows the output when exciter and receiver are separated by an increasing distance of 5 mm each while in trace (b) positions of exciter and receiver are interchanged at $x = 1$ cm.
- Fig. 4 Dispersion curve (experimental curve) at $B = 32$ G.
- Fig. 5 Azimuthal velocity as a function of plasma radius.
- Fig. 6 Radial distribution of space potential at different magnetic fields.
- Fig. 7 Azimuthal velocity as a function of magnetic field. Curve 'a' shows the velocity determined by test wave technique (v_{drift}) curve 'c' represents the velocity measured by Langmuir probe ($V_{\vec{E} \times \vec{B}}$) and curve 'b' represents the corrected $V_{\vec{E} \times \vec{B}}$ which includes the finite Larmor radius correction and effects of cylindrical geometry.
- Fig. 8 Normalized velocity as a function of T (v/Ω_c).

Discharge Arrangement

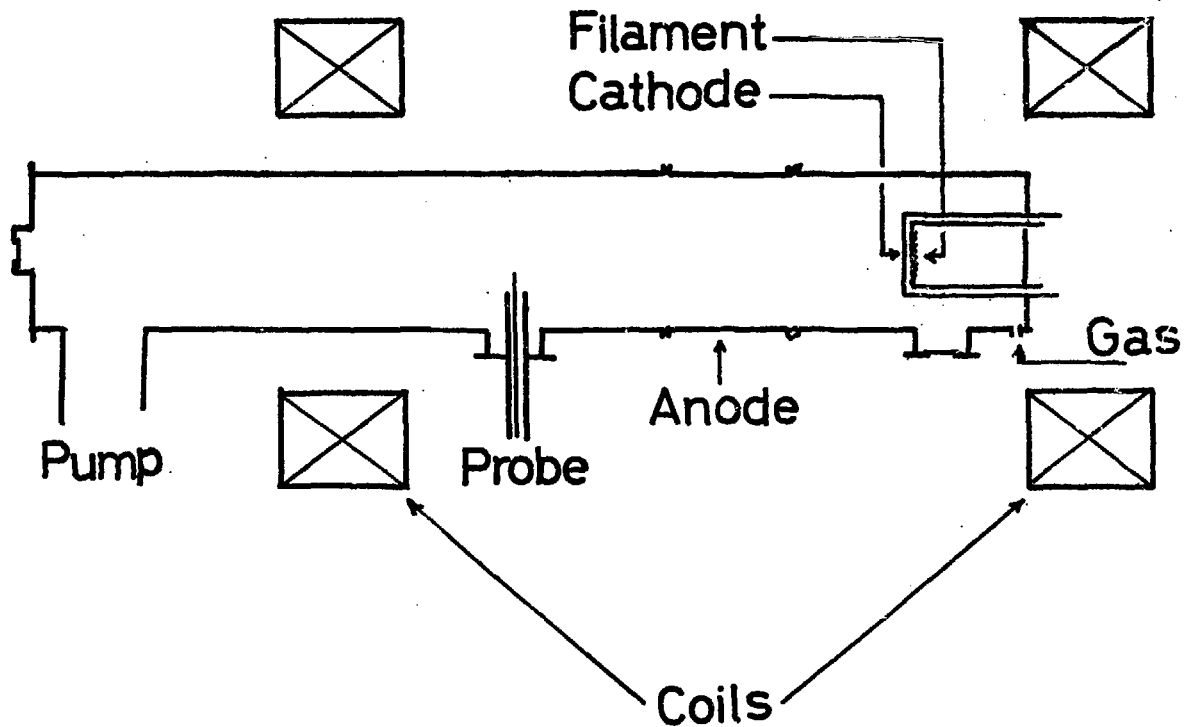


Fig.1

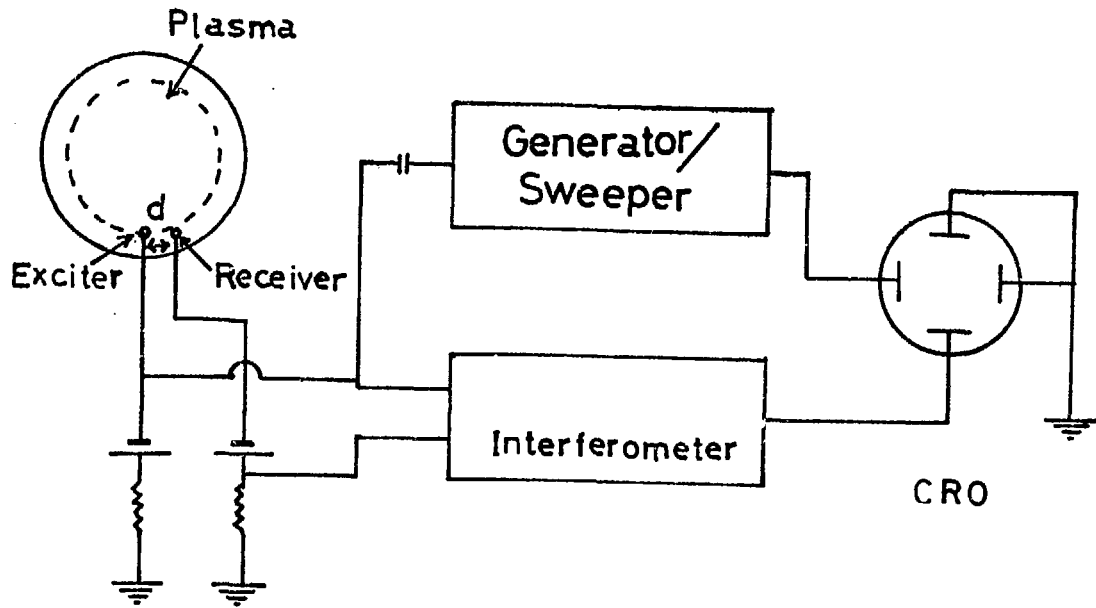
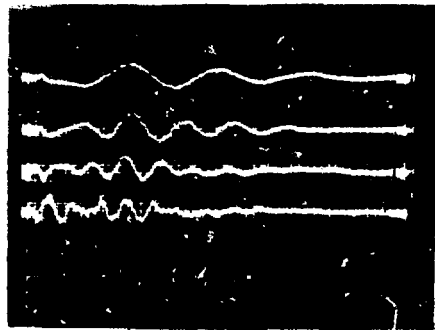
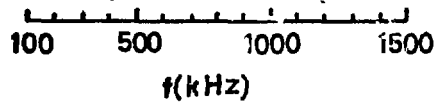


Fig.2



(a)



(b)

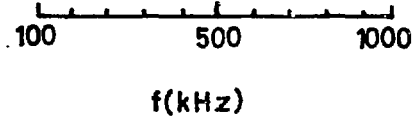


Fig. 3

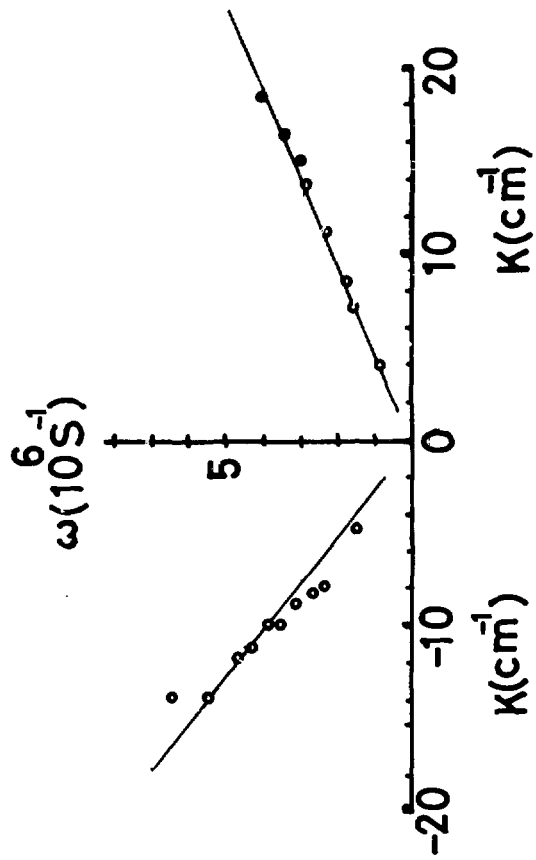


Fig.4

v_{θ} vs r
B = 32 G

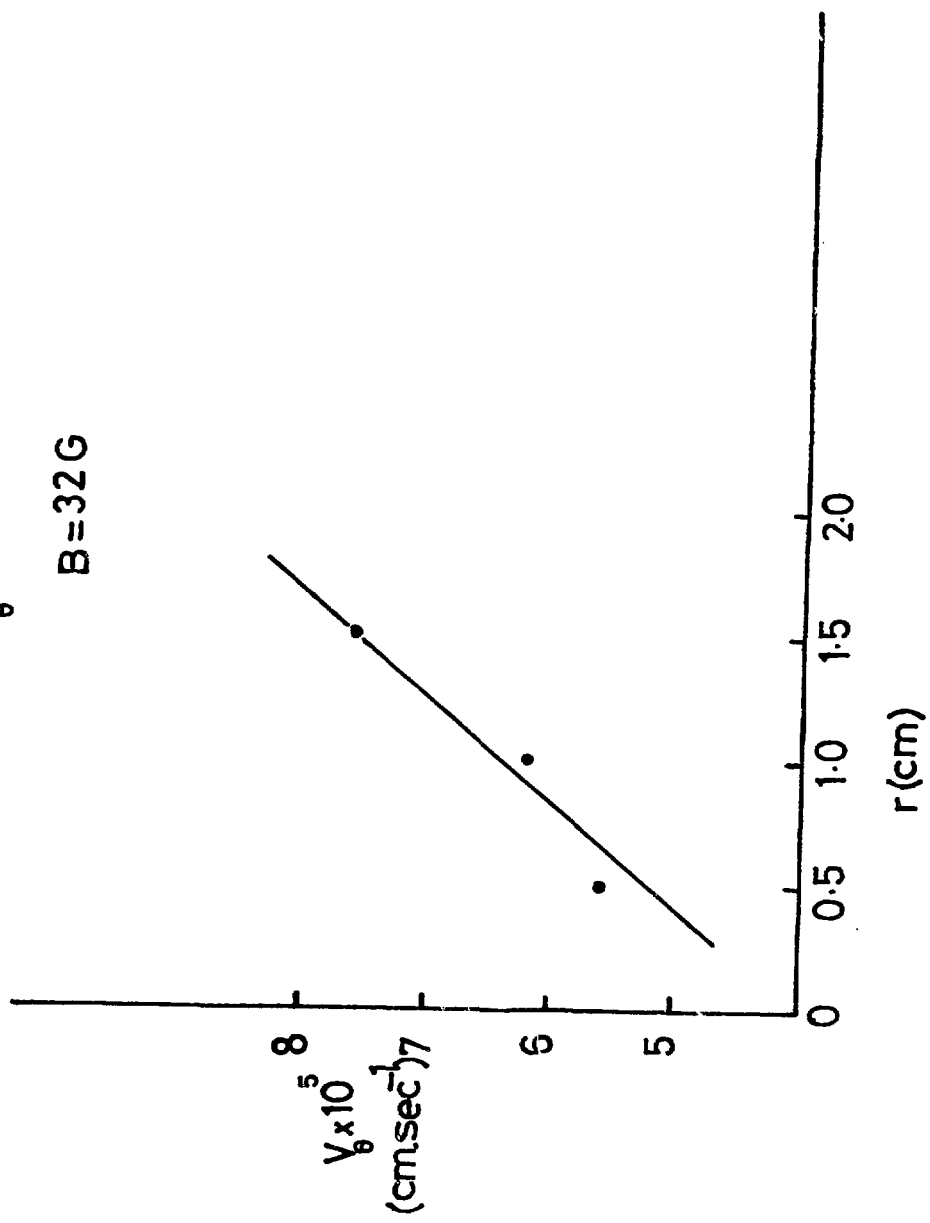


Fig.5

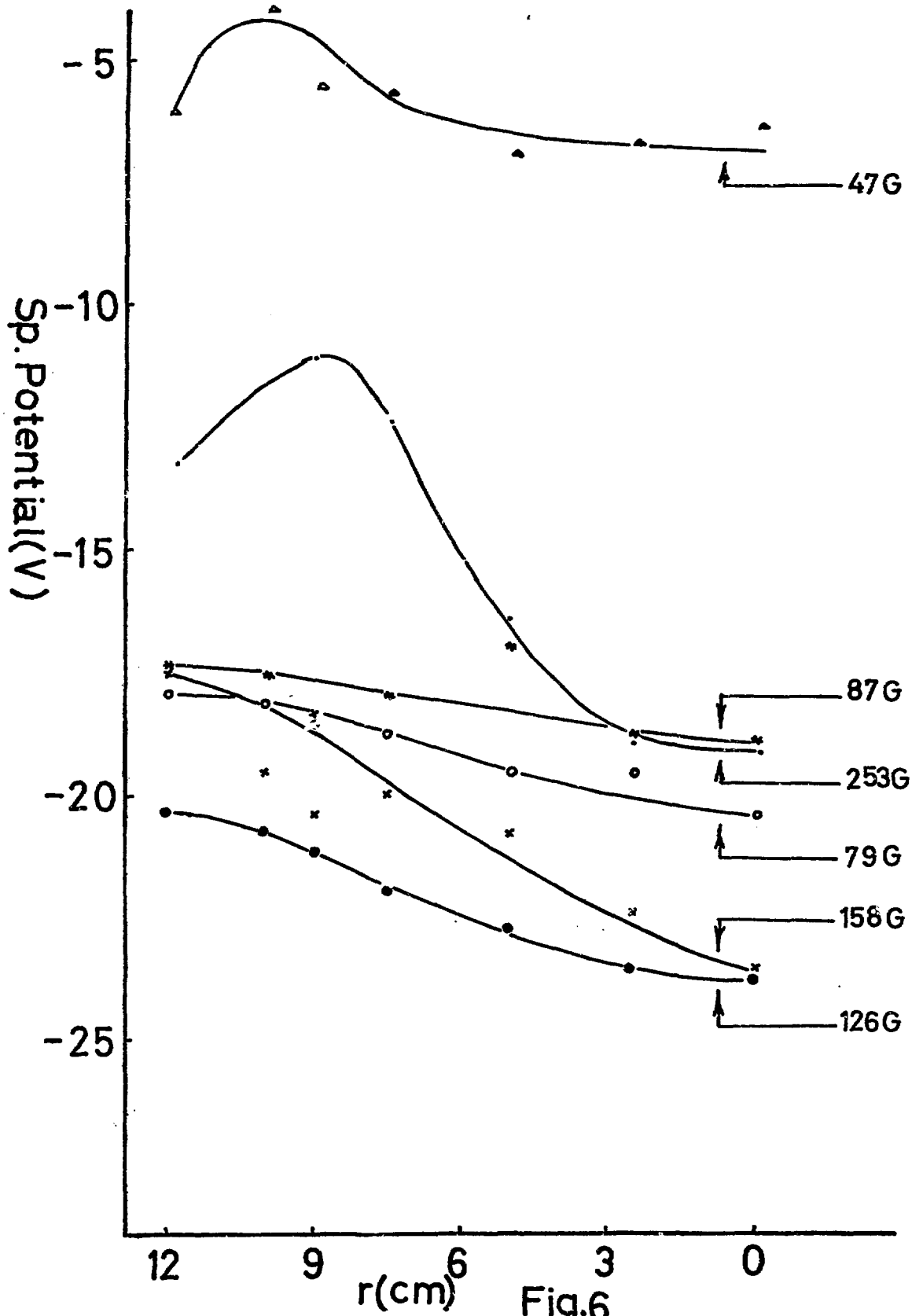


Fig.6

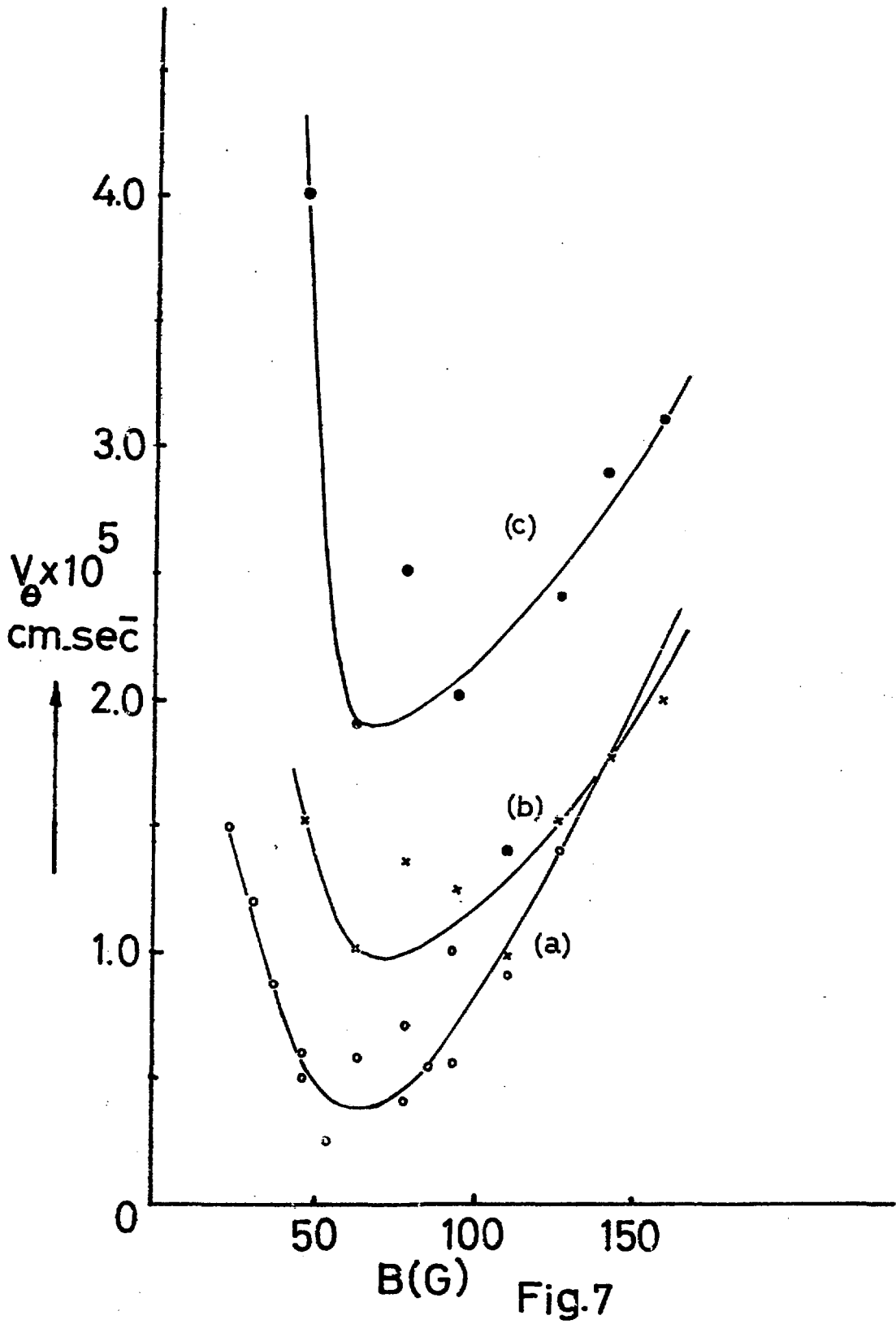


Fig.7

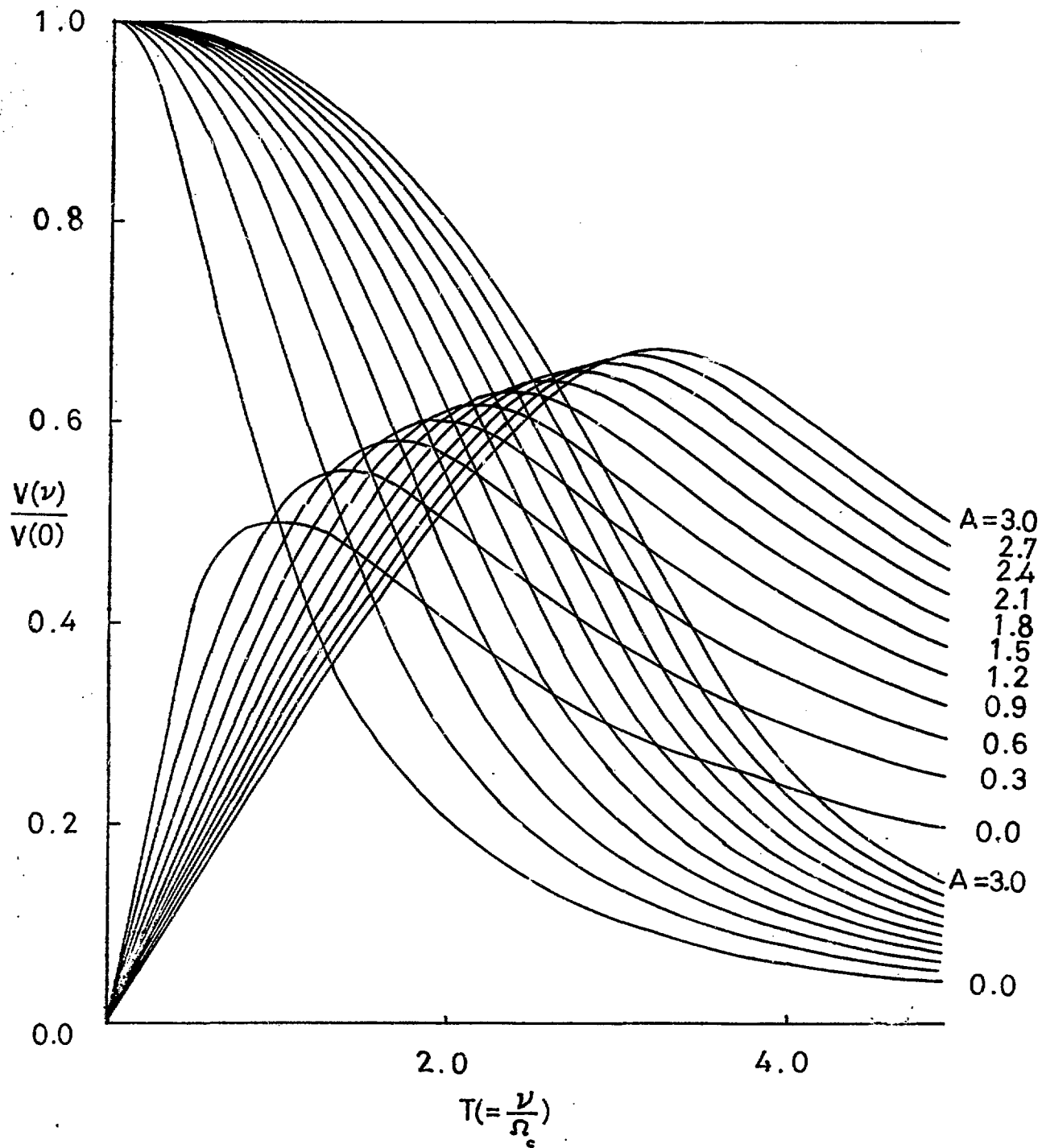


Fig. 8